Journal of Applied Polymer Science

Chitosan-Based Wet-Spun Scaffolds for Bioactive Agent Delivery

Seniz Ucar,[1,2] Pinar Yilgor,[3] Vasif Hasirci,[2,4] Nesrin Hasirci[1,2]

[1]Department of Chemistry, Faculty of Arts and Sciences, Middle East Technical University, 06800 Ankara, Turkey
[2]BIOMATEN, Center of Excellence in Biomaterials and Tissue Engineering, Middle East Technical University, 06800 Ankara, Turkey
[3]Department of Biomedical Engineering, Faculty of Engineering and Architecture, Cukurova University, 01330 Adana, Turkey
[4]Department of Biological Sciences, Faculty of Arts and Sciences, Middle East Technical University, 06800 Ankara, Turkey
Correspondence to: N. Hasirci (E-mail: nhasirci@metu.edu.tr)

ABSTRACT: Use of scaffolds both as supporting materials at defect site and delivery vehicles for bioactive agents is a commonly employed strategy to aid in tissue repair and regeneration. In this study, fibrous meshes of chitosan were prepared by wet spinning and coated with alginate. BSA as a model protein and gentamicin as a model antibiotic were incorporated into the scaffolds in multiple loading models and their release kinetics were studied. The effects of structural form of scaffold and properties of bioactive agents on release profiles were evaluated. Our results suggest that, designed scaffolds are potential candidates for tissue engineering with the feature of controlled bioactive agent delivery. © 2013 Wiley Periodicals, Inc. J. Appl. Polym. Sci. 130: 3759–3769, 2013

KEYWORDS: biomaterials; drug delivery systems; polysaccharides; structure-property relations

Received 31 January 2013; accepted 2 June 2013; Published online 1 July 2013
DOI: 10.1002/app.39629

INTRODUCTION

Tissue repair and regeneration is a complex process that should be managed through meeting the explicit requirements in each case. Use of biodegradable scaffolds functionalized via incorporation of cells or bioactive agents is an advantageous strategy in which scaffolds both act as supporting materials for tissue growth and delivery vehicles for local and controlled administration of bioactive agents.[1]

Using scaffolds for local delivery of bioactive agents in a controlled manner is a common approach to achieve the most beneficial treatment at target site.[2–4] In tissue-engineering applications, antibiotic delivery is aimed for both prophylaxis and treatment purposes against microorganisms, whereas proteins are employed to regulate the progress of repair and regeneration. Gentamicin is a broad-range antibiotic and scaffolds possessing sustained release of gentamicin were demonstrated to show excellent antibacterial properties and potential to treat infections.[5,6] Also, proteins, growth factors and hormones are demonstrated to be highly effective on cellular activities in a time- and concentration-dependent manner and their controlled release from scaffolds have been shown to enhance healing and new tissue formation.[7–11]

Several methods have been established to produce constructs for scaffold-based tissue-engineering applications because architecture of scaffolds is highly effective on their properties.[12–14] Fibrous architecture possesses the advantages of high surface area-to-volume ratio and high and interconnected porosity. These structural characteristics have been shown to provide a favorable environment for cell attachment and cell infiltration, especially by use of microsized fibers.[15] In addition, it was reported that meshes with micronsized fibers create a hydrodynamic microenvironment that eases mass transport, exchange of cell nutrients and wastes.[16] Fiber fabrication techniques include 3D printing and various spinning methods such as wet spinning, dry spinning, melt spinning, gel spinning, jet spinning, and electrospinning. Among these methods, wet spinning is an easily applicable, reproducible, and cost-efficient method that allows the production of microfibers under mild conditions. In tissue-engineering applications, wet-spinning technique has been employed successfully with both synthetic and natural polymers to fabricate scaffolds with defined and controlled fibrous structure.[17,18]

Chitosan (Ch) and alginate are natural polysaccharides proven to be biodegradable, biocompatible, nonantigenic, nontoxic, and biofunctional.[19–21] Inherent osteoconductivity of Ch resulting in enhanced cell adhesion and osteoblastic differentiation has been verified in literature.[22,23] Possessing excellent properties for tissue-engineering applications and being easily processable have

favored Ch and alginate as widely used scaffolding materials either separately or together in their polyelectrolyte complex form.[24–32] Wet-spun Ch and Ch blend scaffolds have also been mentioned in literature for tissue-engineering applications. In addition, incorporation of bioactive agents such as growth factors and anticancer drugs has been reported.[33–39]

In this study, Ch fibrous scaffolds were coated with alginate, for the first time in literature, which contributed to incorporation of bioactive agents in multiple loading models. Effects of both structural form of scaffold and varying properties of bioactive agents on release kinetics were examined. Additionally, scaffolds were characterized in terms of mechanical properties, water uptake and retention capacity, and degradation profiles to be used in tissue-engineering applications.

MATERIALS AND METHODS

Materials

Ch low viscous [≤200 mPa s, 1% (v/v) in 1% (v/v) acetic acid at 20°C; 75–85% deacetylated] was obtained from Fluka (Osaka, Japan) and sodium alginate (from brown algae) was obtained from Sigma-Aldrich (St. Louis, MI). Methanol (free from acetone, pure) and glacial acetic acid were bought from Sigma-Aldrich. Calcium chloride (pure, granular) used as cross-linker was from Riedel De Haen (Seelze, Germany). Bovine serum albumin (BSA) was obtained from Boehringer-Mannheim (Mannheim, Germany) and coomassie plus the better Bradford assay kit was purchased from Thermo Scientific (Rockford, IL). Lysozyme (from chicken egg white, activity of 96,831 U/mg) was bought from Fluka (Bornem, Belgium). Gentamicin was purchased from Ulagay (Istanbul, Turkey).

Preparation of Scaffolds

In order to prepare Ch scaffolds, Ch was first dissolved in 2 vol % aqueous acetic acid to yield 4 wt % solution. Then, 0.6 mL portions of the Ch solution were injected through a needle using a syringe pump at a speed of 5 mL/h (New Era NE-1000, New York), into a coagulation bath of Na_2SO_4 (0.5 M): NaOH (1 M): distilled water (dH_2O) prepared in 3:1:6 (v/v) ratio. Fibers formed were kept in the coagulation bath overnight. They were then washed and incubated in dH_2O for 30 min. In order to dehydrate, fibers were incubated in 50 vol % methanol/water solution for 1 h and pure methanol for 3 h. After completion of the dehydration process, the fibers were manually pressed into plastic cylindrical molds, with diameter of 1.2 cm and height of 1.0 cm, and dried at 54°C for 2 h to form randomly oriented 3D meshes.[33]

Coating of Ch scaffolds with alginate was carried out via vacuum-pressure cycling. For this purpose, Ch scaffolds were put into 24 well-plates and 0.3 mL of 2 wt % aqueous alginate solution was introduced onto each scaffold in 0.1 mL portions followed by vacuum-pressure cycling after every addition. The scaffolds were placed in clean well-plates and stayed for overnight. Stabilization of alginate layer on alginate-coated Ch (Ch/Alg) scaffolds was achieved by ionic cross-linking. For this purpose, 200 μL of ethanol was introduced on Ch/Alg scaffolds by vacuum-pressure cycling. Then, first 1 mL of 10 wt % $CaCl_2$ solution prepared in 75 vol % aqueous ethanol solution and later on 5 wt % aqueous $CaCl_2$ solution were added on each scaffold, followed by vacuum-pressure cycling. Finally, scaffolds were rinsed with excess dH_2O to remove any $CaCl_2$ remaining on the surface and washed with ethanol before drying under vacuum.

Characterization of Scaffolds

Structural Characterization. In order to investigate coating formation, Ch/Alg scaffolds were frozen by immersing in liquid nitrogen and cut into half with a sharp razor. Cross-sectional micrographs of the scaffolds were taken by scanning electron microscopy (SEM; Jeol JSM-6400 Electron Microscope, Tokyo, Japan). Surface composition of both Ch/Alg and Ch single filaments were examined by attenuated total reflectance Fourier transform infrared spectroscopy (ATR-FTIR, Perkin Elmer Spectrum 65, MA). Thickness determination of Ch and alginate-coated Ch fibers was carried out by using light microscopy (Leica TCS SPE, Wetzlar, Germany) and cross-sectional SEM images of the scaffolds.

Water Uptake and Retention Capacity. Dry weights of scaffolds (W_d) were recorded and then, the samples were immersed in dH_2O for 24 h. Scaffolds were weighed at the end of incubation period (W_u) for calculation of percent water uptake values (E_u). In order to determine percent water retention capacity (E_r), each scaffold was placed in a centrifuge tube within a piece of filter paper at the bottom of the tube, and centrifuged at 1000 rpm for 3 min.[40] The samples were weighed after centrifugation (W_r) and values were recorded. Water uptake and retention capacities of scaffolds were investigated for both Ch and Ch/Alg scaffolds and calculated according to following equations:

$$E_u(\%) = \frac{W_u - W_d}{W_d} \times 100 \quad (1)$$

$$E_r(\%) = \frac{W_r - W_d}{W_d} \times 100 \quad (2)$$

Five replicate samples were used for each group.

Degradation of Scaffolds. Degradation behavior of scaffolds was investigated in three different media as dH_2O, phosphate buffer saline (PBS) and enzyme solution. In order to observe degradation behavior in PBS and dH_2O, scaffolds were incubated in 5 mL of PBS (10 m*M*; pH = 7) or dH_2O at 37°C in a shaking water bath. In every 2 days, medium was refreshed. At determined time intervals (3, 7, 14, 21, 28, 35, and 42 days), samples were taken out, rinsed thoroughly with dH_2O, lyophilized, and weighed. Enzymatic degradation behavior of scaffolds was investigated by incubating both Ch and Ch/Alg scaffolds in 5 mL of 1 mg/mL lysozyme solution prepared in PBS (10 m*M*; pH = 7), at 37°C in a shaking water bath. Lysozyme concentration was chosen based on the literature data.[41,42]

Enzyme solutions were refreshed in every 2 days to maintain enzyme activity. At predetermined time intervals (3, 7, 14, 21, 28, 45, and 70 days), samples were taken out, rinsed thoroughly with dH_2O, lyophilized, and weighed. Five replicate samples were used for each group.

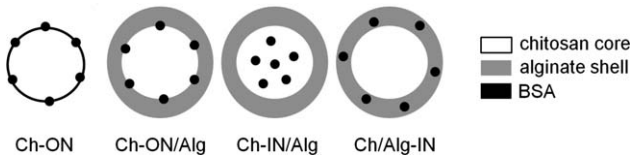

Figure 1. Schematic representation of BSA loading models.

Mechanical Analysis of Scaffolds. The compressive mechanical properties of fibrous scaffolds were studied by using mechanical tester (Lloyd LRX 5K, West Sussex). Prior to testing, the scaffolds were incubated in 1 mL of DMEM high glucose medium, for 24 h at 37°C in a shaker to mimic the biological environment. For compression tests, scaffolds were placed between compression presses and compressed with a rate of 1 mm/min until failure. The compressive moduli of scaffolds were calculated from the initial linear elastic region (E_1) and linear deformation region after strain hardening (E_2) of the resultant stress–strain curves. Also applied stress (σ) values at 20% and 50% strain (ϵ) are measured. Compressive moduli of scaffolds were calculated according to following formula where F is applied force (N), A is area (mm^2), Δl is the change in scaffold thickness (mm), and l_0 is initial thickness (mm).

$$E(\text{MPa}) = \frac{\sigma}{\in} = \frac{F/A}{\Delta l/l_0} \quad (3)$$

Five replicate samples were used for both Ch and Ch/Alg scaffolds in cylindrical shape with a diameter of 0.8 cm and thickness of 0.5 cm.

In Situ Release Studies of Bioactive Molecules. Release kinetics of bioactive molecules from the scaffolds was simulated by using BSA as a model protein and gentamicin as a model antibiotic through incubation of scaffolds in PBS medium (10 m*M*; pH = 7) at 37°C in a shaker bath. BSA release was determined spectrophotometrically by using Bradford Assay and gentamicin release was determined by measuring the absorbance at 256 nm by UV–vis spectrophotometer.

Incorporation of BSA into the Scaffolds. BSA was incorporated into different layers of scaffolds as "ON" and "IN" models in four different loading modes and represented as: Ch–ON, Ch–ON/Alg, Ch–IN/Alg, and Ch/Alg–IN (Figure 1). In "ON" models, 100 μL of 0.5 mg/mL BSA solution was added onto Ch scaffolds and a series of vacuum-pressure cycles were applied. For "IN" models, BSA was added within the polymer solutions of Ch prior to wet spinning or Alg prior to scaffold coating. In each loading model, 50 μg of BSA was incorporated per scaffold.

Incorporation of Gentamicin into the Scaffolds. Gentamicin was loaded either "ON" or "IN" the Ch fibrous mesh scaffolds. Release kinetics was studied from three different loading models represented as: Ch–ON, Ch–ON/Alg, and Ch–IN/Alg. Ch/Alg–IN model was eliminated because of strong ionic interaction between gentamicin and alginate that results in precipitation of the complex and prevent homogeneous mixing. In "ON" models, 100 μL of 20 mg/mL gentamicin solution was added onto Ch scaffolds and a series of vacuum-pressure cycles were applied. For "IN" model, gentamicin was added within the Ch solution prior to wet spinning. In each loading model, 2 mg of gentamicin was incorporated per scaffold.

Antibacterial Tests. Antibacterial activity of gentamicin-loaded scaffolds was examined by disk-diffusion method. For this purpose, *Escherichia coli* (*E. coli*) was spread on agar plates with cotton swabs from bacterial suspensions. Ch–ON and Ch–ON/Alg scaffolds loaded with 100 μg of gentamicin were placed on top of the inoculated agar together with unloaded Ch scaffold as control and 10 μg gentamicin tablet as the standard. The same procedure was also applied on Ch–ON and Ch–ON/Alg scaffolds, which were immersed in PBS for 24 h prior to antibacterial test, to observe maintenance of antibacterial activity with sustained release of antibiotic.[43] The plate was then incubated at 37°C for 24 h. The zones of inhibition indicating the absence of bacteria colonies demonstrated the effect of gentamicin release and its sustained activity.

RESULTS AND DISCUSSION

Scaffold Preparation and Structural Analysis

Two types of scaffolds as Ch and Ch/Alg were prepared by wet spinning of Ch and addition of alginate onto these wet spun meshes to form a coating layer. Ch fibrous meshes were prepared by injection of viscous polymer solution into the coagulation bath that resulted in fiber formation through acid–base precipitation reaction. The concentration and acidity of the Ch solution affecting the viscosity and the spinnability were optimized for proper fiber formation. After injection, Ch fibers were kept in coagulation bath overnight for the precipitation reaction to be completed that occurs initially at the surface of the fibers and proceeds to inner through diffusion, which is called as boundary motion.[44]

Alginate solutions of various concentrations were prepared and 2 wt % concentration in aqueous medium was chosen to be used in coating process because higher concentrations of alginate solution were too viscous that did not enable homogeneous addition by vacuum cycling. Cross-linking of alginate was achieved through linkage of carboxyl groups with divalent Ca^{2+} ions. Among other cations, Ca^{2+} was chosen because it is naturally present in human body. When alginate is directly incubated in aqueous $CaCl_2$ solution for cross-linking, two processes compete with each other that are dissolution of alginate in water and cross-linking of carboxyl ends via Ca^{2+} ion.[45] Therefore, to prevent any loss during cross-linking, scaffolds were first treated with pure EtOH which is a nonsolvent for alginate. Subsequently, they were treated with $CaCl_2$ solution of EtOH–dH_2O mixture and aqueous $CaCl_2$ solution afterwards. Resultant scaffolds were 0.5 cm in thickness and 0.8 cm in diameter. Average weights of the prepared Ch scaffolds and Ch/Alg scaffolds were found to be 22.29 ± 2.18 mg and 26.56 ± 1.78 mg, respectively, demonstrating about 16 wt % alginate in final products.

Microfibrous structure gives scaffold the advantages of high surface to volume ratio and interconnected porosity for improved cell attachment and penetration. In addition, mass transport of cell nutrients, O_2, and wastes is enhanced by simulation of hydrodynamic microenvironment resembling *in vivo*

Applied Polymer SCIENCE

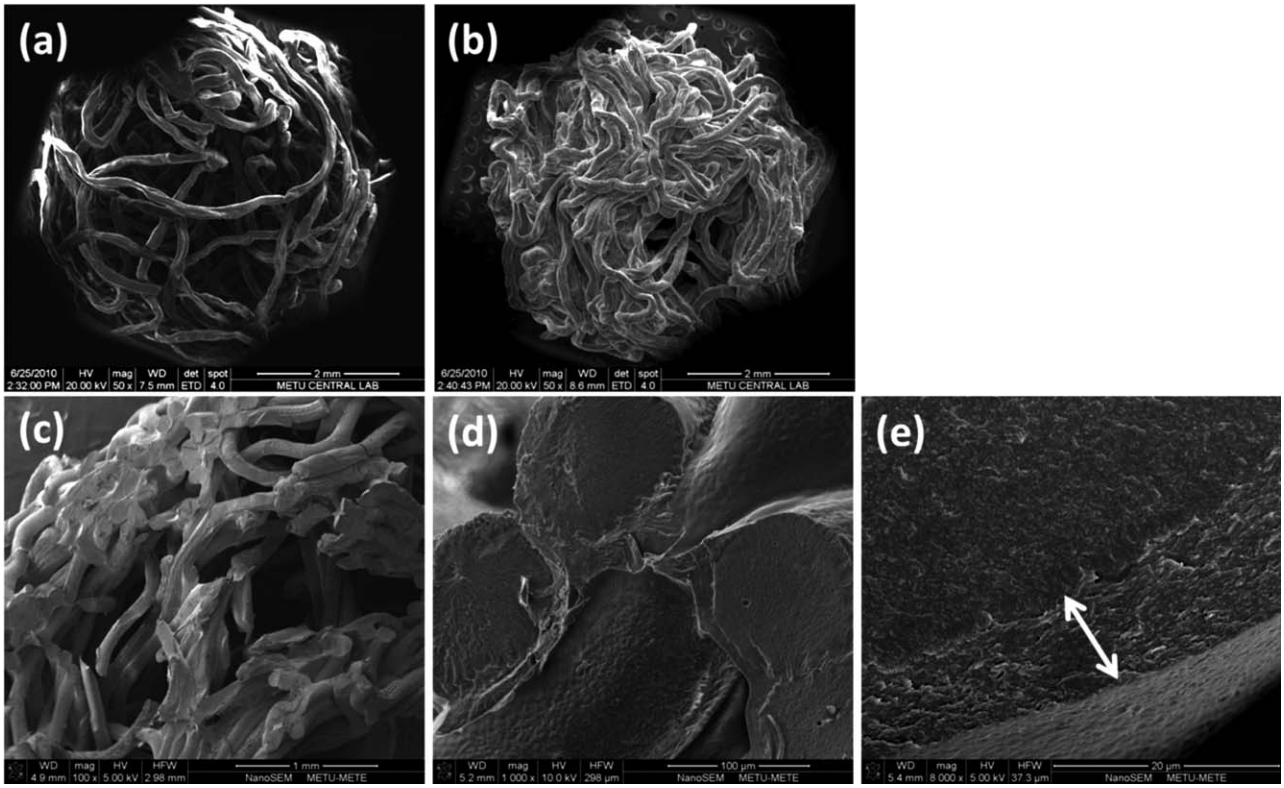

Figure 2. SEM images of (a) Ch scaffold and (b) Ch/Alg scaffold from top, and cross-sectional SEM images of Ch/Alg scaffold (c) ×100, (d) ×1000, and (e) ×8000.

conditions.[15,16] In order to examine the structure of scaffolds, SEM images were used (Figure 2). Ch scaffold was observed to have fibrous structure with high and interconnected porosity. In Ch/Alg scaffold it was observed that upon addition via vacuum cycling, alginate tends to accumulate mostly on Ch fibers as a coat rather than filling up voids, and the fibrous structure was maintained.

Cross-sectional SEM micrographs of Ch/Alg scaffolds also supported that, by addition of alginate in small portions and applying vacuum cycle after each addition, alginate was obtained as a coating layer on Ch fibers without altering fibrous structure and porosity dramatically (Figure 2). By use of light microscopy and SEM images, thickness of Ch fiber and Alg coating were measured to be 93.09 ± 1.58 and 8.51 ± 0.88 μm, respectively. Diameter of Ch fibers was directly affected by needle diameter, coagulation bath, and concentration of polymer solution whereas coating thickness was dependent on concentration and amount of alginate solution introduced on fibers.[46,47]

In addition, FTIR-ATR analyses were conducted on Ch fiber, Ch/Alg fiber and alginate (Figure 3). In the FTIR-ATR spectrum of Ch fiber, two characteristic peaks were observed at 1630 and 1373 cm^{-1} which were attributed to amine vibration and symmetric vibration of CH_3, respectively.[48] When the filaments were treated with alginate, those peaks were replaced by typical absorption bands of alginate detected at 1592 and 1411 cm^{-1} resultant from antisymmetric and symmetric stretching of COO^- groups. Both spectra exhibited peaks around 1020 cm^{-1} that were assigned to skeletal vibrations of C–O–C which exists in the ring structure of both polymers.[49,50] Similarly, OH stretching was observed in both spectra at 3200–3500 cm^{-1} range because of hydroxyl groups of both Ch and alginate. Additionally, in the case of Ch fiber, overlapping of OH stretching with NH stretching resulted in a broader peak at that region.

Because FTIR-ATR has a penetration depth in micrometer scale and after alginate addition characteristic peaks of Ch were replaced by absorption bands corresponding to alginate

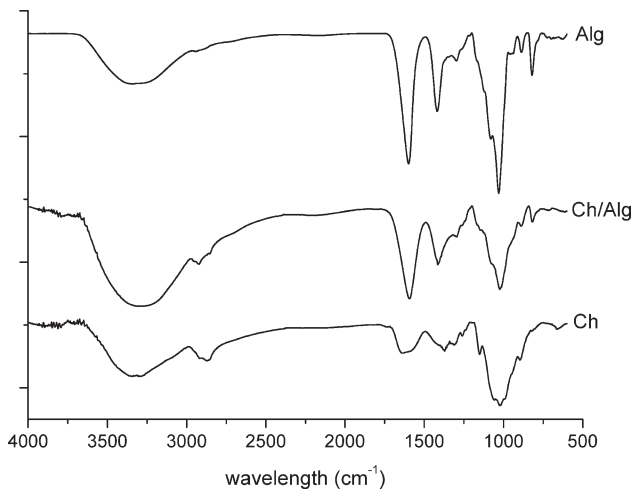

Figure 3. FTIR-ATR spectra of Ch filament, Ch/Alg filament and calcium cross-linked Alg.

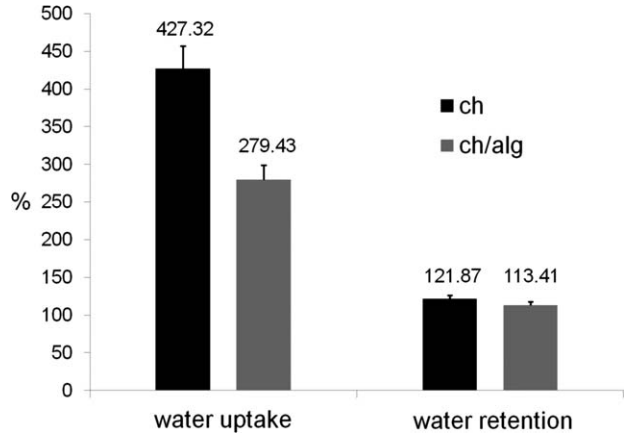

Figure 4. Percent water absorption and retention values for Ch and Ch/Alg scaffolds.

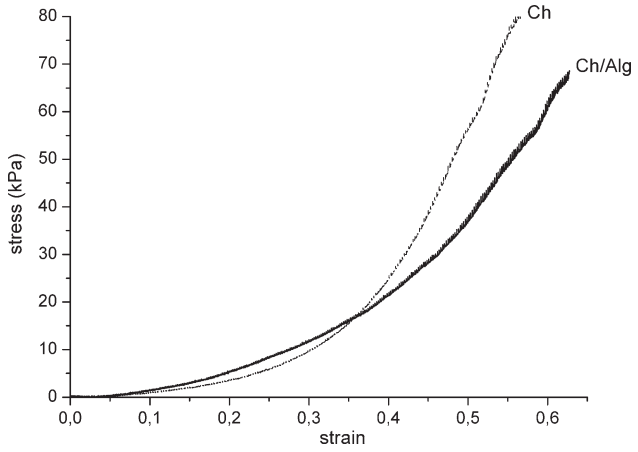

Figure 5. Representative stress–strain curves of scaffolds.

functional groups, it was concluded that upon addition, alginate formed a coating layer on Ch fibers. Absence of characteristic peaks at 1730 and 1530 cm^{-1} corresponding to strong electrostatic interactions between Ch and alginate indicated weak interfacial interaction between layers.

Scaffold Characterization

Absorption of body fluid to all parts of the structure, transfer of nutrients, and metabolic wastes are influenced by water uptake capacity as does the cell attachment and migration all over the scaffold, that eventually affects the morphology of newly grown tissue.[51] Water retention ability on the other hand, was demonstrated to be crucially important for natural tissues especially to maintain their viscoelastic properties.[52] Therefore, both characteristics were evaluated for Ch and Ch/Alg scaffolds to demonstrate their suitability for tissue-engineering applications. After incubation in dH_2O for 24 h, percent water uptake (E_u) and retention (E_r) values for Ch and Ch/Alg scaffolds were obtained by weight measurement (Figure 4). Corresponding percent water uptake values were $427.32 \pm 30.26\%$ and $279.43 \pm 19.70\%$, respectively. Upon incubation, fibrous Ch scaffolds demonstrated excellent water uptake capacity, which was attributed to water absorbed into the dehydrated fibers and adsorbed within the voids of structures. High water uptake ability of Ch on account of its hydrophilic hydroxyl and amino groups has been verified in literature also. Ch scaffolds prepared by freeze-drying were shown to have a water uptake value of 1600% by Thein-Han et. al. and 2000% by Venkatesan et al.[40,53] In conclusion, both chemical characteristics of Ch and highly porous structure of scaffolds were stated as contributors to significant water uptake. Although a remarkable decrease was observed in the case of Ch/Alg scaffolds, they still exhibited high water uptake capacity. Once cross-linked with $CaCl_2$, alginate becomes insoluble in dH_20 and exhibits low water uptake ability that varies with cross-linker concentration and cross-linking time.[54] Therefore, when cross-linked alginate was coated on Ch fibers, access of water to the fibers was blocked to some extent. Additionally, introduction of alginate decreased the volume of void space in the scaffolds. As a result, percent water uptake values were lower for Ch/Alg scaffolds. Water retention capacity was investigated by centrifuging the scaffolds after incubation in dH_2O in order to remove free water from the structures. Ch and Ch/Alg scaffolds were shown to have the capability to retain as much water as their weight with the values of $121.87 \pm 4.44\%$ and $113.41 \pm 4.44\%$, respectively. High water retention capacities of both Ch and alginate were attributed to their chemical structures similar to GAGs, which are dominantly effective on water retention capacity of tissues through their high charge density and inherent hydrophilicity.[55]

Mechanical properties were examined from the compressive stress–strain curves and representative graphs for both Ch and Ch/Alg scaffolds are given (Figure 5). Because of highly porous fibrous structure, initial application of load resulted in compression of pores along with a linear elastic deformation region (E_1). As the stress on scaffolds was increased gradually, closing of pores and enhanced densification resulted in a strain hardening behavior (E_2).[56] Compressive moduli and compressive stress (σ) at 20% and 50% strain for Ch and Ch/Alg scaffolds were calculated and given in Table I.

The compression properties of scaffolds were comparable to many studies reported in literature to be used as biomaterials. Bryant et al.[57] reported PEG hydrogels with compressive modulus of 30–1300 kPa to be used in cartilage tissue engineering. Elastin hydrogels as potential tissue-engineering scaffolds were prepared by Annabi et al.[58] and reported to have compressive

Table I. Compressive Moduli and Stress Values at 20% and 50% Strain for Scaffolds

	E_1 (kPa)	E_2 (kPa)	σ (kPa) at 20% strain	σ (kPa) at 50% strain
Ch	16.77 ± 3.97	344.49 ± 36.94	3.61 ± 0.97	52.76 ± 14.12
Ch/Alg	38.12 ± 9.79	258.51 ± 17.31	5.44 ± 1.19	34.59 ± 4.06

Applied Polymer SCIENCE

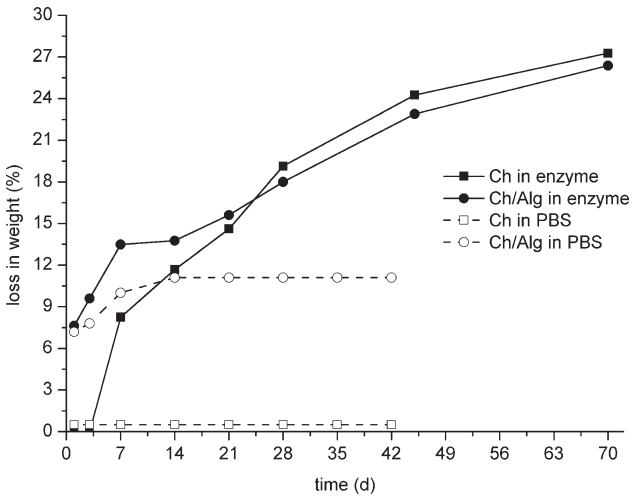

Figure 6. Degradation graphs of Ch and Ch/Alg scaffolds in PBS (dashed lines) and 1 mg/mL lysozyme solution (solid lines).No weight loss was observed in dH_2O for both scaffolds.

modulus of 3.9–18.8 kPa. Porous foams of elastin, having compressive modulus of 6.25–215 kPa over a strain range of 20–80%, were demonstrated to be promising candidates for soft tissue-engineering applications by Srokowski et al.[59] Comparison of E_1 values of Ch and Ch/Alg scaffolds revealed that incorporation of cross-linked alginate into the porous scaffolds resulted in a twofold increase in compressive modulus, mainly by decreasing the void space and porosity within the structure. Compressive strength of Ch/Alg scaffold at 20% strain, laying within the initial elastic deformation region for both kinds of scaffolds, was also measured to be higher. After closing of pores by increased stress, mechanical properties of scaffolds increased tremendously. Ch scaffolds showed higher E_2 values because of superior mechanical characteristics of Ch to alginate. In accordance, the applied stress on Ch scaffolds at 50% strain was higher compared to Ch/Alg scaffolds exhibiting lower E_2.

Degradation of scaffolds was investigated because tissue-engineering scaffolds should be biodegradable to replace with newly forming tissue. In addition, course of degradation, either surface or bulk, and degradation rate highly affect the release behavior and stability of scaffolds. Studies were conducted in dH_2O, PBS, and lysozyme-containing PBS solution (1 mg/mL).

Both Ch and Ca^{2+} cross-linked alginate are insoluble in water, and, neither Ch nor Ch/Alg scaffolds showed any mass loss upon incubation in dH_2O. When the scaffolds were incubated

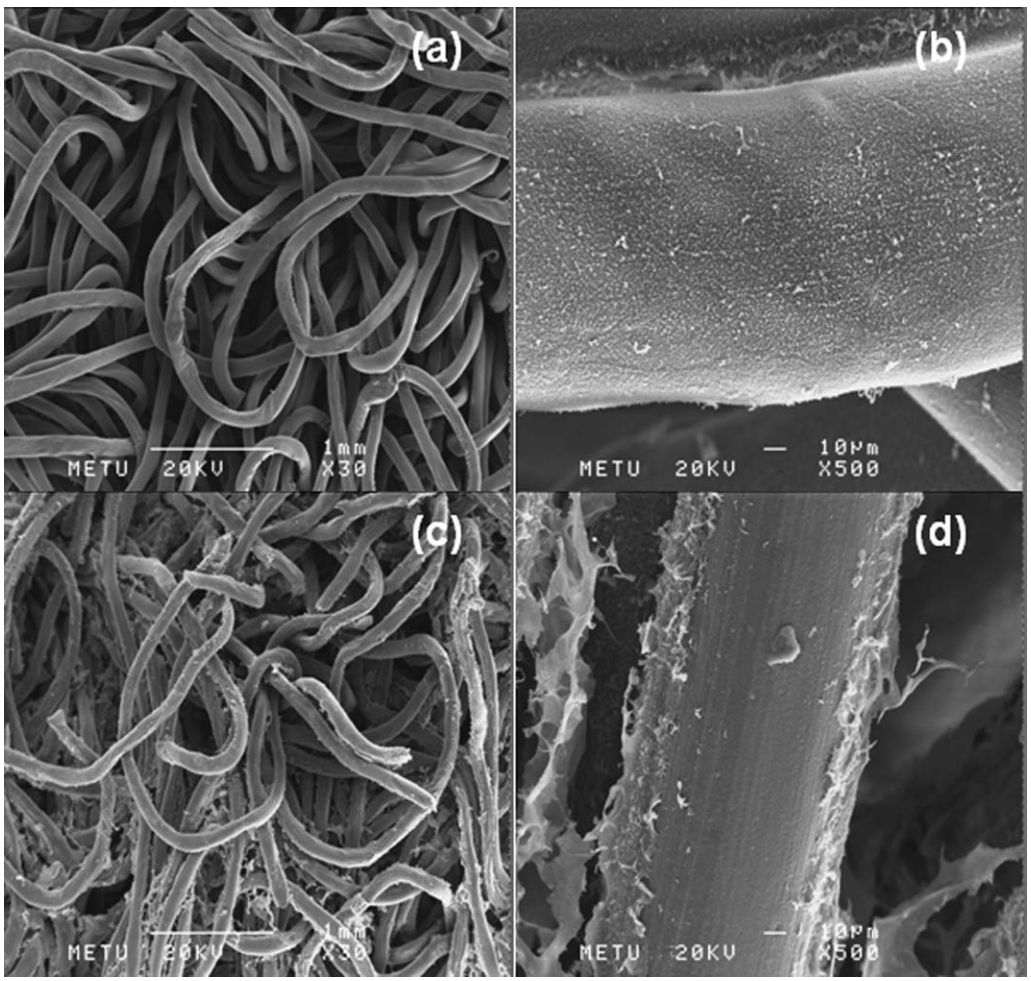

Figure 7. SEM images of (a,b) Ch and (c,d) Ch/Alg scaffolds on third day of incubation in enzyme solution at (a,c) ×30 and (b,d) ×500.

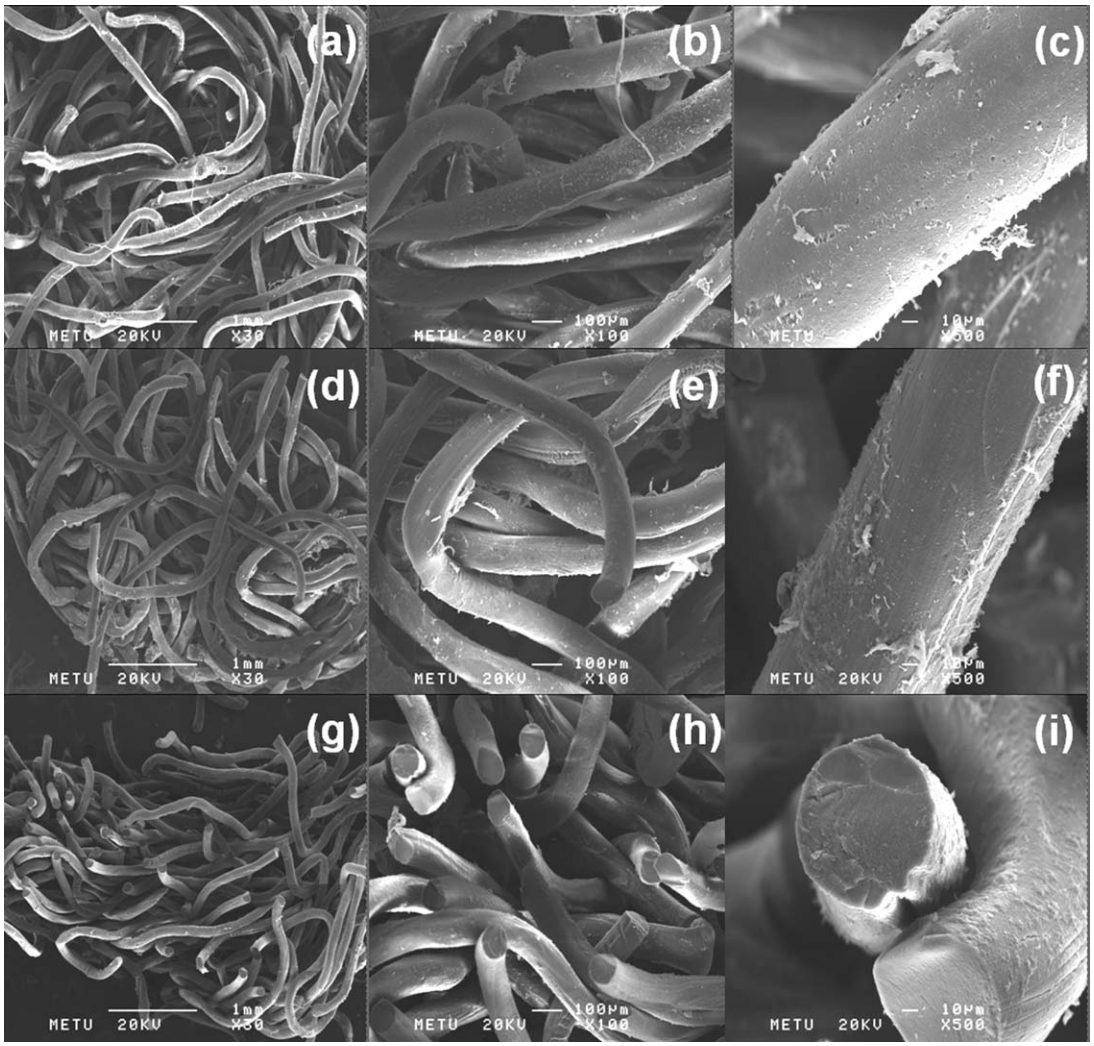

Figure 8. SEM images of (a,b,c) Ch and (d,e,f) Ch/Alg scaffolds from upperview and (g,h,i) Ch scaffolds from cross section on 70th day of incubation at (a,d,g) ×30, (b,e,h) ×100, and (c,f,i) ×500.

in PBS solution, again no mass loss was observed in Ch scaffolds. However, Ch/Alg scaffolds lost 7.20% of their total weight upon 24 h of incubation in PBS and total weight loss increased to 11.1% at 14 days (Figure 6). The decrease in total mass observed in Ch/Alg scaffolds was resultant from the dissolution of alginate layer as ionic cross-linking by Ca^{2+} was subjected to cation exchange with monovalent K^+ and Na^+ ions and subsequent dissolution of alginate.

In vivo, Ch is known to mainly degrade enzymatically by lysozyme which cleaves the glycosidic bonds in polysaccharides. Therefore, incubation of scaffolds in 1 mg/mL lysozyme solution prepared in PBS caused degradation in both kinds of scaffolds that reached a loss of 27% of total weight at 70 days (Figure 6). It was observed that Ch scaffolds showed no degradation during the first 3 days of incubation followed by a fast degradation rate afterwards. However, Ch/Alg scaffolds showed a fast mass loss upon initial incubation resultant from removal of alginate layer because of coactions of PBS dissolution and enzymatic degradation. SEM images of scaffolds taken upon 3 days of incubation in enzyme solution clearly showed the erosion of Ch surface in uncoated scaffolds and removal of alginate layer from coated ones (Figure 7).

In order to examine the course of degradation, SEM images of enzymatically degraded scaffolds were taken from upper view and cross section at the end of incubation period of 70 days (Figure 8). SEM micrographs revealed the surface erosion of fibers clearly, whereas bulk integrity was preserved. Scaffolds were able to maintain their structural unity and stability up to 70 days in enzyme medium. As a result, it was concluded that scaffolds undergo surface degradation and could provide support at defect site for a prolonged time during repair and regeneration process.

Release Studies

Two bioactive model agents, BSA and gentamicin were loaded on or in the scaffolds and their release studies were carried out.

BSA Release

BSA release studies showed that up to first 6 h of incubation a fast release was observed for all models because of initial rapid water uptake and release of the surface-adsorbed molecules,

Applied Polymer SCIENCE

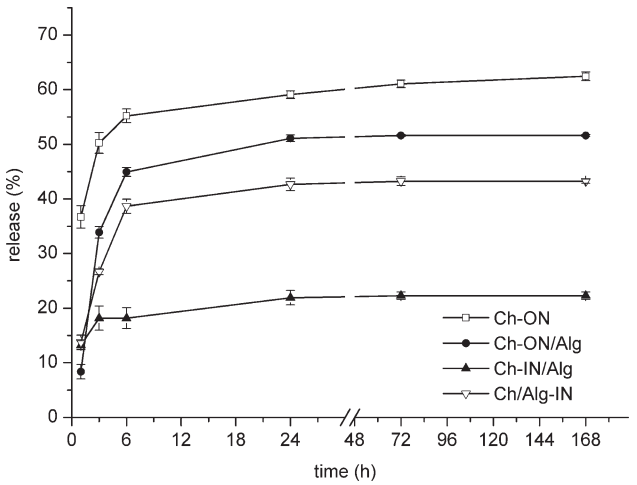

Figure 9. Release of BSA from scaffolds in 7 day period.

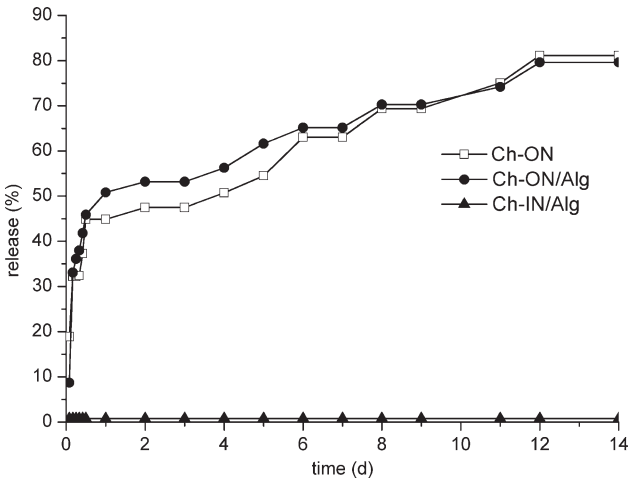

Figure 10. Release profiles of gentamicin from scaffolds.

which slowed down afterwards (Figure 9). From day 3–7, release of BSA continued with a slow rate and very slow release was observed after day 7. Ch–ON, Ch–ON/Alg, and Ch/Alg–IN models showed efficient release profiles with varying burst release characteristics. However, in Ch–IN/Alg model total BSA release remained quite low.

Fastest release of BSA was observed in uncoated Ch–ON model as expected because of direct release of surface-adsorbed BSA into the incubation medium. The maximum amount of release was reached in that model also with 62.47 wt %. In Ch–ON/Alg model where alginate coating was introduced, total amount of BSA release was 51.63 wt %. Comparison of BSA release profiles from Ch–ON and Ch–ON/Alg models revealed that alginate coating was efficient in decreasing the burst release of BSA during the first 6 h of incubation. As incubation period was prolonged, release rates in both models became comparable to each other. The retarding effect of alginate layer on BSA release was lost because of dissolution of ionically cross-linked alginate as seen in degradation studies.

In Ch/Alg–IN model, where BSA is loaded within alginate coating, release was achieved by diffusion and dissolution of alginate. Total release was found to be 43.24 wt %, which is lower compared to Ch–ON models of either uncoated or alginate-coated scaffolds. In Ch–ON models, BSA was introduced onto the neutral Ch core and adhered to the surface. When incubated in PBS they were easily desorbed. On the other hand, when introduced into the alginate solution, electrostatic interactions between the oppositely charged amino acids and the anionic polysaccharide macromolecules may have partially restrained the release of BSA. Ch–IN/Alg model exhibited the slowest and lowest amount of total release for BSA with a value of 22.31 wt %. In literature, previous studies of BSA release from Ch substrates also demonstrated low burst release followed by poor release profiles because of strong charge interactions between Ch solution and BSA, and high molecular weight of BSA that restricts its diffusion.[60,61] Initial release of BSA from Ch–IN/Alg model was attributed to desorption of protein molecules, which were on the outer shell of fibers so could be released into the medium. Consequently, low release of BSA from Ch–IN/Alg model was attributed to entrapment of large BSA molecules within the fibers via structural restrictions and chemical interactions.

For all loading models, burst followed by very slow release was observed in PBS media. The burst is expected because the BSA molecules attaching to the surface by adsorption or stay there without having any attraction would release immediately. The following release should be a diffusion-controlled process. However, a significant sustained release profile could not be obtained because of the strong interactions between the protein and Ch molecules. However, as it was shown in degradation studies, Ch was stable in PBS but was subjected to surface degradation in enzyme presence. Therefore, *in vivo* conditions where enzyme is present, degradation of Ch fibers would occur leading to faster release of trapped BSA molecules compared to PBS media.

Gentamicin Release

In the case of tissue-engineering applications, the most advantageous release profile for antibiotics is a burst release followed by a sustained release period.[62] Such kind of a release profile was obtained for gentamicin when Ch–ON and Ch–ON/Alg models were used (Figure 10).

It was observed that 45 wt % of loaded gentamicin was released upon 12 h of incubation and 80 wt % recovery of totally loaded drug by release was achieved in 12 days in both Ch–ON and Ch–ON/Alg models. The fast release of gentamicin seen in the first 12 h of incubation was resultant from the rapid water uptake of scaffolds and dissolution of the antibiotic at the surface by a diffusion-controlled mechanism. In their study, Ji et al.[63] also showed a similar release behavior for gentamicin from Ch nanoparticles and attributed the initial fast release to easy diffusion of surface drugs first followed by diffusion from matrix. Results showed that alginate coating had little effect on slowing the burst release of gentamicin only upon 2 h of incubation. Then, release profiles showed nearly equality for both Ch and Ch/Alg scaffolds. Because gentamicin is a small molecule, it was easily diffused into the incubation medium despite of the alginate layer as it swells and dissolves readily in PBS. No release of gentamicin was observed from Ch–IN/Alg model.

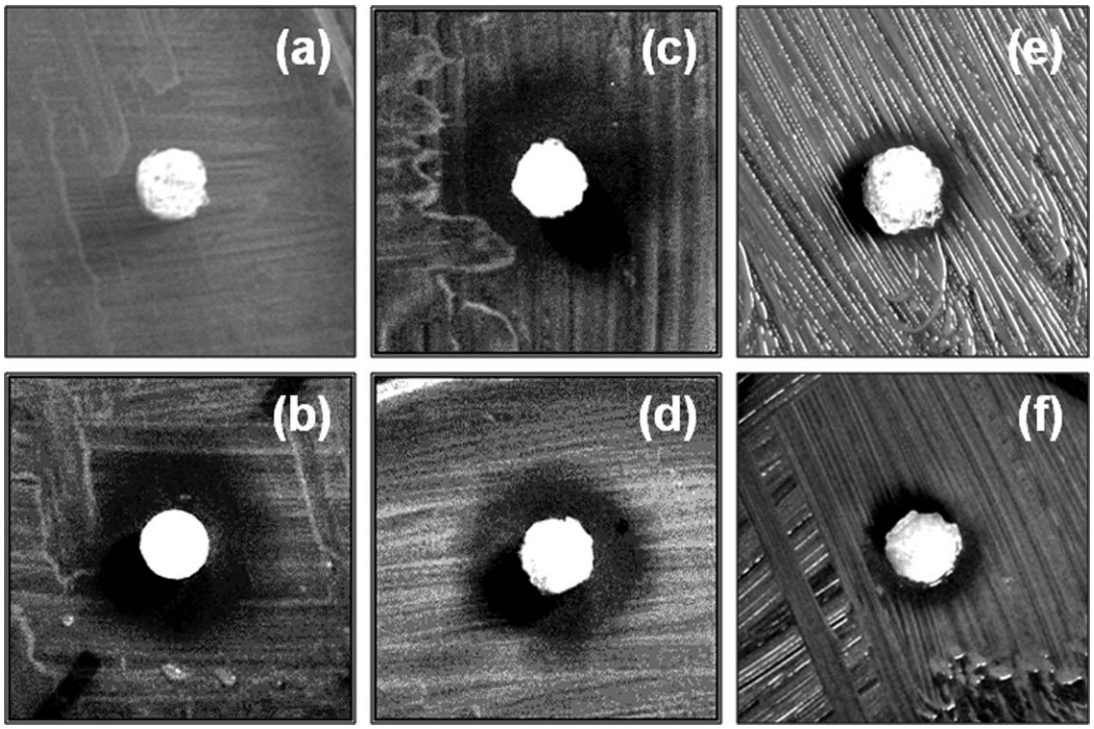

Figure 11. Photograph of E. *coli*-spreaded agar plate after incubation at 37°C for 24 h; (a) Ch, (b) gentamicin tablet, (c) Ch-ON, (d) Ch-ON/Alg; and after immersion in PBS for 24 h and then incubation in agar plate; (e) Ch-ON, (f) Ch-ON/Alg.

Further investigation during scaffold preparation procedure revealed that 51.59 wt % of loaded gentamicin was released into the coagulation bath during incubation of fibers after wet spinning and 20.41 wt % was released into dH_2O during washing process. An additional 9.12 wt % of loaded gentamicin was lost in dehydration procedure. As a result, 81.12 wt % of totally loaded drug was observed to be lost throughout the preparation of scaffolds. Therefore, it was concluded that the use of Ch–IN/Alg model scaffolds was not efficient for local administration of antibiotics that are small molecules easily diffusing out during incubation periods.

Antibacterial Effect of Gentamicin

In order to investigate the antibacterial effect of gentamicin upon release from loaded scaffolds, disk diffusion method was used. Upon incubation of scaffolds at 37°C for 24 h, inhibition zones indicating the antibiotic activity against *E. coli* were observed (Figure 11).

Ch scaffold [Figure 11(a)] used as control showed no inhibition against *E. coli* that was spread over the agar plate. Ch is known to have intrinsic antibacterial activity because of its polycationic nature through interaction of positively charged amino groups with anionic components of cell surface proteins of microorganisms. However, its antibacterial activity is on its surface, therefore, did not cause any inhibition zone on agar plate. On the other hand, gentamicin-containing scaffolds of Ch–ON [Figure 11(c)] and Ch–ON/Alg [Figure 11(d)] models resulted in formation of inhibition zones similar to gentamicin tablet used as standard on the plate. Long-term antibacterial effect of released gentamicin was studied for the same model scaffolds which were immersed in PBS for 24 h and washed (to eliminate the effect of burst release) prior to the antibacterial tests. Inhibition zones were observed for both Ch–ON [Figure 11(e)] and Ch–ON/Alg [Figure 11(f)] scaffolds with smaller diameter because of lower concentration of antibiotic present in the matrices. From these results, it was concluded that antibacterial activity of gentamicin was preserved throughout the drug loading and release periods and both models of scaffolds can be successfully used for gentamicin delivery.

CONCLUSION

In this study, it was aimed to design polymeric scaffolds that would exhibit optimal properties to be used in tissue-engineering applications with the feature of controlled bioactive agent delivery. Ch-based scaffolds were produced by wet-spinning method that resulted in porous, microfibrous structure and alginate coating was introduced as a contributing layer for loading and regulation of release kinetics of bioactive agents. Characterization of scaffolds by means of mechanical properties and degradation profiles demonstrated their capability to be used in tissue-engineering applications.

Effects of loading model and nature of bioactive agent on release kinetics were studied. Results showed that structural hindrance mediated by either introduction of an additional coating layer or loading of drug within the polymer matrix ("IN" models) resulted in lower release profiles compared to uncoated and 'ON' models. Meanwhile, the extent of release also varied for bioactive agents depending on their properties such as net charge and molecular weight. In case of alginate coating,

decrease in burst release of BSA up to 6 h of incubation and insignificant retarding effect for gentamicin release was observed.

When charges of molecules are considered at pH 7, gentamicin is positively charged whereas BSA with pI 4.7 is negatively charged. However, results showed that polyanionic alginate layer was much more effective on slowing down the release of BSA molecules. Thus, the disparity in release profiles were dominantly attributed to the drastic difference between molecular weights of antibiotic and protein molecules (e.g., 560 Da for gentamicin and 66 kDa for BSA). Because release of agents from scaffolds was achieved via diffusion-controlled mechanism, size of bioactive molecules became the dominant factor affecting release rate and gentamicin release from all scaffolds proceeded faster than BSA release because of its smaller molecular weight. Resultant scaffolds are concluded to be potential candidates for tissue-engineering applications with tunable drug delivery characteristics.

ACKNOWLEDGMENTS

The authors would like to thank the financial support from the Office of Scientific Research Projects Coordination of METU.

REFERENCES

1. Fisher, M. B.; Mauck, R. L. *Tissue Eng. Pt B. Rev.* **2013**, *19*, 1.
2. Kologlu, M. B.; Bahadır, G. B.; Vargun, R.; llkay, H.; Bagrıacik, E. U.; Yolbakan, S.; Guven, C.; Endogan, T.; Hasirci, N.; Dindar, H. *J. Urol.* **2010**, *75*, 223.
3. Gunbas, I. D.; Sezer, U. A.; Gulce, S.; Deliloglu, I. G.; Hasirci, N. *Ind. Eng. Chem. Res.* **2012**, *51*, 11946.
4. Mourino, V.; Boccaccini, A. R. J. R. *Soc. Interface* **2009**, *7*, 209.
5. Balmayor, E. R.; Baran, E. T.; Azevedo, H. S.; Reis, R. L. *Carbohyd. Polym.* **2012**, *87*, 32.
6. Lee, D. W.; Yun, Y. P.; Park, K.; Kim, S. E. *Bone* **2012**, *50*, 974.
7. Kanczler, J. M.; Ginty, P. J.; White, L.; Clarke, N. M. P.; Howdle, S. M.; Shakesheff, K. M.; Oreffo, R. O. C. *Biomaterials* **2010**, *31*, 1242.
8. Yilgor, P.; Sousa, R. A.; Reis, R. L.; Hasirci, N.; Hasirci, V. *J. Mater. Sci. Mater. M.* **2010**, *21*, 2999.
9. Dyondi, D.; Webster, T. J.; Banerjee, R. *MRS Proc.* **2011**, 1312.
10. Hunziker, E. B.; Enggist, L.; Küffer, A.; Buser, D.; Liu, Y. *Bone* **2012**, *51*, 98.
11. Kim, S.; Kang, Y.; Krueger, C. A.; Sen, M.; Holcomb, J. B.; Chen, D.; Wenke, J. C.; Yang, Y. *Acta Biomater.* **2012**, *8*, 1768.
12. Marcos-Campos, I.; Marolt, D.; Petridis, P.; Bhumiratana, S.; Schmidt, D.; Vunjak-Novakovic, G. *Biomaterials* **2012**, *33*, 8329.
13. Yu, X.; Xia, Z.; Wang, L.; Peng, F.; Jiang, X.; Huang, J.; Rowe, D.; Wei, M. *J. Mater. Chem.* **2012**, *19*, 9721.
14. Oliveira, A. L.; Sun, L.; Kim, H. J.; Hu, X.; Rice, W.; Kluge, J.; Reis, R. L.; Kaplan, D.L. *Acta Biomater.* **2012**, *4*, 1530.
15. Puppi, D.; Dinucci, D.; Bartoli, C.; Mota, C.; Dini, F.; Barsotti, G.; Carlucci, F.; Chiellini, F. *J. Bioact. Compat. Pol.* **2011**, *26*, 478.
16. Gomes, M. E.; Sikavitsas, V. I.; Behravesh, E.; Reis, R. L.; Mikos, A. G. *J. Biomed. Matter. Res. A* **2003**, *67*, 87.
17. Puppi, D.; Piras, A. Chiellini, M. F.; Chiellini, E.; Martins, A.; Leonor, I. B.; Neves, N.; Reis, R. L. *J. Tissue Eng. Regen. M* **2011**, *4*, 253.
18. Hwang, C. M.; Park, Y.; Park, J. Y.; Lee, K.; Sun, K.; Khademhosseini, A.; Lee, S. H. *Biomed Microdevices* **2009**, *11*, 739.
19. Burke, A.; Yilmaz, E.; Hasirci, N. *J. Appl. Polm. Sci.* **2002**, *84*, 1185.
20. Leonor, I. B.; Rodrigues, M. T.; Gomes, M. E.; Reis, R. L. *J. Tissue Eng. Regen. M* **2011**, *2*, 104.
21. Burke, A.; Yilmaz, E.; Hasirci, N. *Turk J. Med. Sci.* **2000**, *30*, 341.
22. Li, Z.; Ramay, H. R.; Hauch, K. D.; Xiao, D.; Zhang, M. *Biomaterials* **2005**, *26*, 3919.
23. Mathews, S.; Gupta, P. K.; Bhonde R.; Totey, S. *Cell Proliferat.* **2011**, *44*, 537.
24. Alsberg, E.; Anderson, K. W.; Albeiruti, A.; Franceschi, R. T.; Mooney, D. J. *J. Dent. Res.* **2001**, *80*, 2025.
25. Turco, G.; Marsich, E.; Bellomo, F.; Semeraro, S.; Donati, I.; Brun, F.; Grandolfo, M.; Accardo, A.; Paoletti, S. *Biomacromolecules* **2009**, *10*, 1575.
26. De la Riva, B.; Nowak, C.; Sánchez, E.; Hernández, A.; Schulz-Siegmund, M.; Pec, M. K.; Delgado, A.; Évora, C. *Biopharm.* **2009**, *73*, 50.
27. Florczyk, S. J.; Kim, D. J.; Wood, D. L.; Zhang, M. *J. Biomed. Mater. Res. A.* **2011**, *98*, 614.
28. Tanase, C. E.; Popa M. I.; Verestiuc, L. *Mater. Lett.* **2011**, *65*, 1681.
29. Beherei, H. H.; El-Magharby, A.; Abdel-Aal, M. S. *Der Pharma Chem.* **2011**, *3*, 10.
30. Isikli, C.; Hasirci, V.; Hasirci, N. *J. Tissue Eng. Regen. M.* **2012**, *6*, 135.
31. Li, B.; Li, L.; Zhou, C. *Appl. Mech. Mater.* **2012**, *140*, 38.
32. Tsai, W. B.; Chen, Y. R.; Li, W.T.; Lai, J. Y.; Liu, H. L. *Carbohyd. Polym.* **2012**, *89*, 379.
33. Tuzlakoglu, K.; Alves, C. M.; Mano, J. F.; Reis, R. L. *Macromol. Biosci.* **2004**, *4*, 811.
34. Tuzlakoglu, K.; Reis, R. L. *J. Mater. Sci.* **2007**, *18*, 1279.
35. Shim, I. K.; Lee, S. Y.; Park, Y. J.; Lee, M. C.; Lee, S. H.; Lee, J. Y.; Lee, S. J. *J. Biomed. Mater. Res. A.* **2008**, *84*, 247.
36. Yilgor, P.; Tuzlakoglu, K.; Reis, R. L.; Hasirci, N.; Hasirci, V. *Biomaterials* **2009**, *30*, 3551.
37. Pati, F.; Adhikari, B.; Dhara, S. *J. Biomat. Sci. Polym. E* **2012**, *23*, 1923.
38. Pati, F.; Adhikari B.; Dhara, S. *J. Mater. Sci.* **2012**, *23*, 1085.
39. Denkbas, E. B.; Seyyal, M.; Piskin, E. *J. Member Sci.* **2000**, *172*, 33.

40. Thein-Han, W. W.; Mısra, R. D. K. *Acta Biomater.* **2009**, *5*, 1182.
41. Kucharska, M.; Walenko, K.; Butruk, B.; Brynk, T.; Heljak, M.; Ciach, T. *Mater. Lett.* **2010**, *64*, 1059.
42. Martins, A. M.; Pham, Q. P.; Malafaya, P. B.; Raphael, R. M.; Kasper, F. K.; Reis, R. L.; Mikos, A. G. *Tissue Eng. Pt. A* **2009**, *15*, 1953.
43. Lee, D.; Cohen, R. E.; Rubner, M. F. *Langmuir* **2005**, *21*, 9651.
44. Knaul, J. Z.; Creber, K. A. M. *J. Appl. Polym. Sci.* **1997**, *66*, 117.
45. Rhim, J. W. *Food Sci. Technol. Int.* **2004**, *37*, 323.
46. Wan, Y.; Cao, X.; Zhang, S.; Wang, S.; Wu, Q. *Acta Biomater.* **2008**, *4*, 876.
47. Matsuda, A.; Ikoma, T.; Kobayashi, H.; Tanaka, J. *Mater. Sci. Eng. C* **2004**, *24*, 723.
48. Wang, Q.; Dong, Z.; Du, Y.; Kennedy, J. F. *Carbohyd. Polym.* **2007**, *69*, 336.
49. Tam, S. K.; Dusseault, J.; Polizu, S.; Ménard, M.; Hallé, J. P.; Yahia, L. H. *Biomaterials* **2005**, *26*, 6950.
50. Lawrie, G.; Keen, I.; Drew, B.; Chandler-Temple, A.; Rintoul, L.; Fredericks, P.; Grøndahl, L. *Biomacromolecules* **2007**, *8*, 2533.
51. Yeo, M. G.; Kim, G. H. *Chem. Mater.* **2012**, *24*, 903.
52. Badylak, S. F.; Freytes, D. O.; Gilbert, T. W. *Acta Biomater.* **2009**, *5*, 1.
53. Venkatesan, J.; Qian, Z. J.; Ryu, B.; Kumar, N. A.; Kim, S. K. *Carbohyd. Polym.* **2011**, *83*, 569.
54. Remuñán-López, C.; Bodmeier, R. *J. Control Rel.* **1997**, *44*, 215.
55. Lovekamp, J. J.; Simionescu, D. T.; Mercuri, J. J.; Zubiate, B.; Sacks, M. S.; Vyavahare, N. R. *Biomaterials* **2006**, *27*, 1507.
56. Oliveira, A. A. R.; Carvalho, S. M.; Leite, M .F.; Orefice, R. L.; Pereira, M.M. *J. Biomed. Mater. Res. B* **2012**, *100*, 1387.
57. Bryant, S. J.; Anseth, K. S. *J. Biomed. Mater. Res. A* **2002**, *59*, 63.
58. Annabi, N.; Mithieux, S. M.; Boughton, E. A.; Ruys, A. J.; Weiss, A. S.; Dehghani, F. *Biomaterials* **2009**, *30*, 4550.
59. Srokowski, E. M.; Woodhouse, K. A. *J. Biomat. Sci. Polym. E* **2008**, *19*, 785.
60. Xu, Y.; Du, Y. *Int. J. Pharm.* **2003**, *250*, 215.
61. Xu, Y.; Zhan, C.; Fan, L.; Wang, L.; Zheng, H. *Int. J. Pharm.* **2007**, *336*, 329.
62. Zilberman, M.; Elsner, J. J. *J. Control Rel.* **2008**, *130*, 202.
63. Ji, J.; Hao, S.; Wu, D.; Huang, R.; Xu, Y. *Carbohyd. Polym.* **2011**, *85*, 803.